Published OnlineFirst on October 2, 2012; DOI:10.1158/1078-0432.CCR-12-1876

Clinical Cancer Research

Establishment and Characterization of Novel Cell Lines from Sinonasal Undifferentiated Carcinoma

Yoko Takahashi, Michael E. Kupferman, Diana Bell, et al.

Clin Cancer Res Published OnlineFirst October 2, 2012.

Published OnlineFirst on October 2, 2012; DOI:10.1158/1078-0432.CCR-12-1876

Human Cancer Biology

Clinical Cancer Research

Establishment and Characterization of Novel Cell Lines from Sinonasal Undifferentiated Carcinoma

Yoko Takahashi[1], Michael E. Kupferman[1], Diana Bell[2], Tilahun Jiffar[1], June Goo Lee[1], Tong-Xin Xie[1], Ning-Wei Li[1,4], Mei Zhao[1], Mitchell J. Frederick[1], Alexander Gelbard[3], Jeffrey N. Myers[1], and Ehab Y. Hanna[1]

Abstract

Purpose: Sinonasal undifferentiated carcinoma (SNUC) is a rare and aggressive cancer. Despite the use of multimodality treatment, the overall prognosis remains poor. To better understand the biologic features of SNUC and help develop new therapies for the disease, we established SNUC cell lines and characterized their biologic behaviors.

Experimental Design: Cell lines were established from a patient with a T4N0M0 SNUC of the right maxillary sinus who was treated with surgical resection at our center. Tumor colonies were harvested and were sequentially replated onto larger plates. Two populations were developed and labeled MDA8788-6 and MDA8788-7. These cell lines were characterized with molecular, biomarker, functional, and histologic analyses.

Results: Short tandem repeat genotyping revealed that the cell line is isogenic to the parental tumor, and cytogenetic analysis identified 12 chromosomal translocations. The SNUC cell lines do not form colonies in soft agar but are tumorigenic and nonmetastatic in an orthotopic mouse model of sinonasal cancer. Western blot analysis revealed that both MDA8788 cell lines express epithelial markers but do not express mesenchymal markers or the endocrine marker synaptophysin.

Conclusions: This is the first report of the establishment of stable human-derived SNUC cell lines. The lines were highly tumorigenic and maintain the histologic and molecular features of the original tumor. These cell lines should serve as useful tools for the future study of SNUC biology and the development and testing of novel therapies for this deadly disease. *Clin Cancer Res; 18(22); 1–10. ©2012 AACR.*

Introduction

Sinonasal undifferentiated carcinoma (SNUC) is a rare, highly aggressive cancer that arises in the nasal cavity and paranasal sinuses. Initially described by Frierson and colleagues in 1986 (1), this tumor is on the spectrum of neuroendocrine sinonasal malignancies, which includes esthesioneuroblastoma, neuroendocrine carcinoma, and small cell carcinoma. There is a male predominance [2-3:1], and there are no known etiologic factors. SNUC is typically negative for Epstein-Barr virus (2, 3). In general, SNUC presents as large tumors involving multiple sinonasal structures, often extends into the orbital or cranial cavity, and can metastasize to the cervical lymph nodes, lungs, bones, brain, and liver (2, 4–6).

The treatment of SNUC includes aggressive multimodal therapy with radiotherapy and chemotherapy and, in some instances, surgery (4, 6–8). Despite aggressive management, the prognosis remains poor, and the median survival time from diagnosis is less than 18 months (2, 3).

To better understand the biologic features of SNUC and help develop new therapeutic strategies for this disease, establishing a reliable model for laboratory-based analysis is essential. While other sinonasal malignancy models have been described, these are not relevant to the biologic characteristics of SNUC (9, 10). In this report, we describe the establishment and characterization of the first human SNUC cell line and present the molecular and phenotypic behavior of this unique system.

Materials and Methods

Primary tumor

A 74-year-old woman was diagnosed and treated at The University of Texas MD Anderson Cancer Center (MDACC; Houston, TX) for a T4N0M0 SNUC of the right maxillary sinus. She had received induction chemotherapy with 4 cycles of etoposide and carboplatin with a partial response

Authors' Affiliations: Departments of [1]Head and Neck Surgery and [2]Pathology, The University of Texas MD Anderson Cancer Center; [3]Department of Otolaryngology-Head & Neck Surgery, Baylor College of Medicine, Houston, Texas; and [4]Department of Nasopharyngeal Carcinoma, Sun Yat-sen University Cancer Center, State Key Laboratory of Oncology in South China, Guangzhou, China

Note: Supplementary data for this article are available at Clinical Cancer Research Online (http://clincancerres.aacrjournals.org/).

Corresponding Author: Michael E. Kupferman, Department of Head and Neck Surgery, The University of Texas MD Anderson Cancer Center, 1400 Pressler, Unit 1445, Houston, TX 77030. Phone: 713-794-1910; Fax: 713-794-4662; E-mail: mekupfer@mdanderson.org

doi: 10.1158/1078-0432.CCR-12-1876

Published OnlineFirst on October 2, 2012; DOI:10.1158/1078-0432.CCR-12-1876

Translational Relevance

Sinonasal undifferentiated carcinoma (SNUC) is a rare, highly aggressive cancer that arises in the nasal cavity and paranasal sinuses. Treatment of SNUC includes aggressive multimodality therapy, including chemoradiotherapy and surgical resection when needed. Despite aggressive management, the prognosis remains poor, and the median survival time is less than 18 months. Because of the rarity of this disease, few studies on SNUC have been conducted, and most of these are focused upon improved diagnostic accuracy. To understand the biologic characteristics of SNUC and to develop novel alternative treatments, it is essential to establish a reliable and phenotypically accurate tumor model system for SNUC. Here, we report the establishment and characterization of two novel SNUC cell lines that are highly tumorigenic and maintain the histologic and molecular features of the original tumor. These cell lines may serve as useful tools for the future study of SNUC and in the development and testing of novel therapies for this deadly disease.

before undergoing surgical resection of the residual tumor. Under an approved Institutional Review Board protocol, a portion of the resected specimen and matching normal tissue were collected.

Ultrastructural characterization of the SNUC specimen

Transmission electron microscopy was conducted by the High Resolution Electron Microscopy Facility at MDACC. A sample was taken from the central portion of the solid tumor from the sinonasal cavity specimen immediately after surgical extirpation and was preserved in a solution containing 3% glutaraldehyde, 2% formaldehyde, and 0.1 mol/L cacodylate (pH 7.3). Ultrathin sections were cut with an LKB Ultracut microtome (Leica), stained with uranyl acetate and lead citrate in an LKB Ultrostainer, and examined with a JEM 1010 transmission electron microscope (JEOL) at an accelerating voltage of 80 kV. Digital images were obtained using the AMT imaging system (Advanced Microscopy Techniques Corp.).

Establishing SNUC cell lines from the patient's tumor

The resected specimen was rinsed in PBS containing 500 units of penicillin and 500 μg of streptomycin and was then rinsed in PBS 3 times. The specimen was minced into 1- to 2-mm^3 pieces and cultured in Dulbecco's Modified Eagle's Medium (DMEM; Invitrogen Corporation) containing 10% FBS (Sigma-Aldrich), 25 units of penicillin, and 25 μg of streptomycin. After 1 month, about 40 tumor colonies were harvested using 3 MM Whatman paper soaked with 0.05% trypsin, 0.0076% EDTA 4Na solution in PBS. The colonies were then transferred to 24-well plates and designated as passage 0. Once the passage 0 cells became confluent, they were sequentially replated. Because they were sensitive to regular trypsin-EDTA solution, the cells were treated with TrypLE Express Stable (Invitrogen) when they were expanded. Cells were maintained in 10% FBS DMEM containing 0.1 mg/mL of Primocin (InvivoGen). Two populations originally from independent colonies were designated MDA8788-6 and MDA8788-7 on the basis of their initial colony numbers. Both the MDA8788-6 and MDA8788-7 lines were free from mycoplasma and murine pathogens by the Infectious Microbe PCR Amplification Test (University of Missouri, Research Animal Diagnostic Laboratory, Columbia, MO).

Acquired cell lines and cell culture

Three established human head and neck squamous carcinoma cells lines were used, UMSCC33, OSC19, MDA1386LN, and an established cancer-associated fibroblast cell line. All cell lines were grown on tissue culture dishes in DMEM supplemented with 10% heat-inactivated FBS.

Short tandem repeat genotyping

The genomic DNA from the acquired cell lines and from the original fresh-frozen tissues were extracted using the Gentra Puregene Cell Kit (Qiagen, Inc.) following the manufacturer's instructions. Short tandem repeat (STR) genotyping was conducted by the Characterized Cell Line Core Facility at MD Anderson.

Karyotyping

G-banding and spectral karyotyping were conducted by MD Anderson's Molecular Cytogenetics Facility by using the following procedures.

Chromosome preparation. Exponentially growing cells were exposed to colcemid (0.04 μg/mL) for 25 minutes at 37°C and hypotonic treatment (0.075 mol/L KCl) for 20 minutes at room temperature. Cells were fixed in a methanol and acetic acid (3:1 by volume) mixture for 15 minutes and washed 3 times in the fixative. The slides were air dried and processed for G-banding and spectral karyotyping.

G-banding. G-banding was conducted by treating the slides in trypsin and staining with Giemsa stain using a routine laboratory procedure (11) to characterize the cytogenetic alterations. Slides were analyzed using an Eclipse E400 microscope (Nikon Inc.), and images of metaphases were captured using an Applied Spectral Imaging system equipped with camera and karyotyping software. A minimum of 15 to 20 metaphases were karyotyped from each sample.

Spectral karyotyping. Spectral karyotyping was conducted according to the manufacturer's protocol using human SKY Paint probes (Applied Spectral Imaging). Images were captured using a Nikon 80i microscope equipped with SKY software (Applied Spectral Imaging). At least 15 to 20 metaphases were analyzed in detail.

Cell proliferation assay

MDA8788 cells were plated on a 96-well plate at a density of 1×10^4 to 2×10^4 per well. After 3, 24, 48, 72, 96, and 120

Published OnlineFirst on October 2, 2012; DOI:10.1158/1078-0432.CCR-12-1876

hours, the culture media were removed; 100 μL of double distilled water was added; and the plates were frozen and thawed 3 times. A total of 100 μL of Hoechst 33342 solution (20 μmol/L in 10 mmol/L Tris-HCl, 2 mol/L NaCl, 1 mmol/L EDTA, pH 7.4; Invitrogen) was added and measured at 360 nm excitation and 460 nm emission. The proliferation data were analyzed using GraphPad Prism 5 (GraphPad Software, Inc.).

Soft agar colony formation assay

Ten thousand MDA8788 cells were suspended in 0.3% agarose (Lonza Walkersville, Inc.) in DMEM containing 20% FBS. This suspension was overlaid onto a solid layer of 0.6% agarose in a 6-well plate. The cells were treated with fresh DMEM containing 20% FBS every other day. Three weeks later, the cells were fixed with methanol, stained with 0.02% crystal violet, and photographed at ×10 magnification.

Anoikis assay

For determination of anoikis resistance, 2×10^6 viable MDA8788 cells were cultured as previously described (12).

Migration and invasion assays

Migration and invasion assays were conducted as previously described (13) using OSC19 cells as a positive control. Briefly, 4×10^4 cells were plated on cell culture insert wells or Matrigel-coated wells (BD Biosciences) in DMEM containing 10% FBS, and the degree of migration was determined after 48 hours.

Protein analysis

The cells from all lines (MDA8788-6, MDA8788-7, MDA1368LN, OSC19, UMSCC33, and cancer-associated fibroblasts) were lysed in lysis buffer (50 mmol/L HEPES, 150 mmol/L NaCl, 10 mmol/L EDTA, 10% glycerol, 1% Triton X-100, pH 7.5) with proteinase inhibitors (1 mmol/L sodium orthovanadate, 1 mmol/L phenylmethylsulfonyl fluoride, ×1 Complete protease inhibitor cocktail; Roche Holding, Inc.). Organ homogenates in TNN buffer [50 mmol/L Tris-HCl (pH 7.4), 150 mmol/L NaCl, 5 mmol/L EDTA, 0.5% Nonidet P-40] were clarified by centrifugation (total lysate). Antibodies were obtained as follows: pan-keratin (clone 80; Thermo Fisher Scientific), cytokeratin 8 (N1N3; GeneTex, Inc.), cytokeratin 19 (Ab-1, clone A53-B/A2.26; Thermo Fisher Scientific), vimentin (clone V9; DAKO), E-cadherin (clone 36/E-cadherin; BD Biosciences), N-cadherin (clone 32; BD Biosciences), synaptophysin (clone SVP-38; Millipore), and actin and α-smooth muscle (SMA; clone 1A4; Sigma-Aldrich).

Immunohistochemical analysis

Immunohistochemistry was conducted as previously described (14), using Cytokeratin Cocktail (mixture of clone AE1/AE3, DAKO; clone CAM 5.2, BD Biosciences; MNF116, DAKO; and clone Zym 5.2, Invitrogen), anti-E-cadherin (clone HECD-1; Invitrogen), anti-α-SMA (clone 1A4; Sigma-Aldrich), and anti-vimentin (clone V9; DAKO).

Animal care

Male nude mice (aged 6–8 weeks) were purchased from the Animal Production Area of the National Cancer Institute-Frederick Cancer Research and Development Center (Frederick, MD). The mice were maintained in a pathogen-free environment and fed irradiated mouse chow and autoclaved reverse osmosis–treated water at facilities in accordance with current regulations and standards of the U.S. Department of Agriculture, U.S. Department of Health and Human Services, and the NIH. The mice were used in accordance with MD Anderson's Animal Care and Use Guidelines, and all animal procedures were done in accordance with a protocol approved by the institution's Institutional Animal Care and Use Committee.

Subcutaneous flank model

A total of 7 or 8 mice per cell line underwent subcutaneous injection with 1×10^6 cells suspended in a volume of 200 μL of PBS directly into the right flank with a 1-mL tuberculin syringe (Hamilton Co.) and a 30-gauge hypodermic needle. The same number of the cells suspended in a volume of 100 μL of PBS with 100 μL of Matrigel Matrix Growth Factor Reduced (BD Bioscience) were also injected into the left flank of the same mice because Matrigel is known to enhance the tumorigenicity of a wide range of cancer cell lines *in vivo* (15). Injected mice were then examined twice weekly for tumor development. When present, tumors were measured using calipers in cephalad-to-caudad and left-to-right dimensions. Tumor volume was calculated as $V = AB^2\ (\pi/6)$, where A is the longest dimension of the tumor and B is the dimension of the tumor perpendicular to A. When the longest dimension reached 15 mm, the animals were euthanized with CO_2. At the time of death, the tumors and lungs were harvested and placed in 10% buffered formalin solution overnight for fixation. Hematoxylin and eosin (H&E) staining was used on histologic sections.

Orthotopic skull base model

We used the soft palate model that was established in our group (16). Briefly, 1×10^6 MDA8788-6 cells were suspended in a volume of 15 μL of PBS with 15 μL Matrigel and injected into the muscle of the soft palate. To monitor orthotopic tumor growth *in vivo*, mice were examined by MRI after 12 days of the injection in the Small Animal Imaging Facility at MDACC. Anesthesia was induced using 5% isoflurane in oxygen, maintained using 1% to 3% in oxygen, and monitored according to respiratory rate using respiratory bellows and a small animal physiological monitoring system (Small Animal Instruments Inc.). All MRIs were acquired using a 7-T Biospec small animal imaging system (Bruker BioSpin) and imaging gradients with an inside diameter (ID) of 116 mm. A linear volume resonator (72-mm ID) was used for excitation, and a custom electronically tuned and actively decoupled RF surface coil (13 mm ID) was used for signal detection. Scout images to verify animal positioning were

Published OnlineFirst on October 2, 2012; DOI:10.1158/1078-0432.CCR-12-1876

followed by high-resolution sagittal T_2-weighted RARE scans [TE/TR 60/3,000 ms, 20 × 15 mm^2 field of view (FOV), 256 × 128 image matrix, 1 mm slices, RARE factor 8, 5 averages], geometrically matched axial T_1-weighted spin echo (TE/TR 11.5/1,000 ms, 20 × 15 mm^2 FOV, 256 × 128 image matrix, 1 mm slices) and T_2-weighted RARE images (TE/TR 60/3,000 ms, RARE factor 8, 5 averages) of the paramedian dorsal skin.

Images were viewed using ParaVision software (Bruker BioSpin) and ImageJ analysis software (rsb.info.nih.gov/ij/). Measurements were taken after comparison of T_1 and T_2 images to confirm consistency of cutaneous microanatomic strata. All measurements were taken using ParaVision software on representative T_2-weighted axial slices.

We euthanized mice with CO_2 when they became moribund. At the time of death, the full heads of mice were obtained, fixed in formalin solution for 48 hours, decalcified in 5% formic acid for 4 days, and paraffin-embedded. H&E staining was done on histologic sections of the head to determine the extent of tumor growth and the degree of invasion into surrounding structures.

Statistical analysis

The unpaired 2-tailed t test was used to compare the differences in mean tumor volume between 2 groups (with or without Matrigel for the tumor injection) with GraphPad Prism 5. $P < 0.05$ was considered statistically significant.

Results

Histopathologic and genetic characteristics

Pathologic analysis of the original tumor was conducted and compared with the established cell lines. H&E staining of the primary tumor from the patient's biopsy showed small- to medium-sized polygonal cells that formed nests, sheets, ribbons, and trabeculae (Fig. 1A), characteristic of the classical SNUC morphology. (1) After the induction chemotherapy, the tumor had developed a slight squamoid appearance (Fig. 1B). Electron microscopy indicated undifferentiated polygonal cells with sparse intracellular membrane structures, as well as ribosomes, neurosecretory granules, and lipid-filled vacuoles (Fig. 1C, left); higher magnification showed that microtubules were present along with rough endoplasmic reticulum, polyribosomes, and membrane-bound, dense-core neurosecretory granules (Fig. 1C, right). The established cell lines grew as adherent and tightly packed monolayers with a polygonal shape and large nuclei (Fig. 1D). The morphology was maintained across all cell passages. STR fingerprinting was conducted to characterize the isogenic nature of the MDA8788 cell lines to the parent tumor. All DNA extracted from the original specimen and the 2 new lines had identical STRs (Supplementary Table).

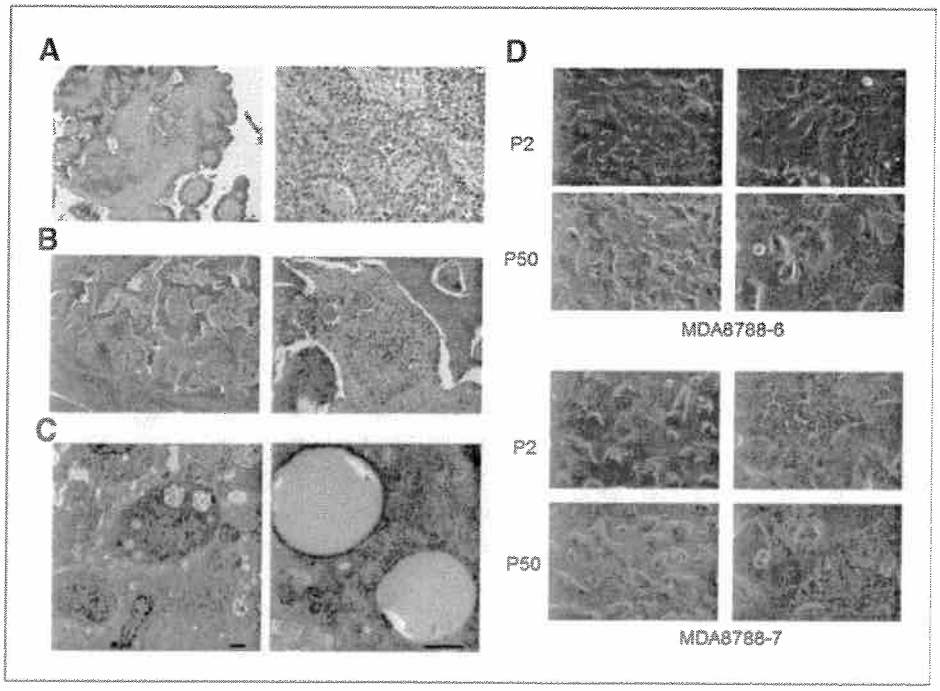

Figure 1. Histopathologic characteristics of the original SNUC and cell morphology of MDA8788-6 and -7 cells. A, H&E staining of the primary tumor from biopsy shows typical features of SNUC, with small- to medium-sized polygonal cells that form nests, sheets, ribbons, and trabeculae [original magnifications, ×40 (left) and ×200 (right)]. B, after induction chemotherapy, H&E staining of the tumor revealed a more squamoid morphology [original magnifications ×40 (left) and ×200 (right)]. C, electron microscopy images. Left, neurosecretory granules, lipid-filled vacuoles, and ribosomes are visible (scale bar, 200 μm). Right, greater magnification reveals rough endoplasmic reticulum and polyribosomes (scale bar, 500 nm). D, each cell line was photographed at both ×40 (left) and ×100 (right) magnification at passages 2 and 50. From early to late passage, both lines maintained a similar morphologic appearance with adherent tightly packed, polygonal-shaped cells with large nuclei growing as a monolayer.

Published OnlineFirst on October 2, 2012; DOI:10.1158/1078-0432.CCR-12-1876

Comparison to the American Type Culture Collection STR database and STR data from 49 cell lines in our laboratory revealed that MDA8788 is a unique cell line, distinct from all others in our collection.

Cytogenetic analysis

Cytogenetic analysis of the MDA8788 cells was conducted by using G-banding and spectral karyotyping analysis. G-banding analysis revealed that 12 clonal markers (m1–m12; Fig. 2A and Supplementary Fig. S1) were shared by both cell lines. By combining G-banding and spectral karyotyping analysis (Fig. 2B), the following translocations were identified: m1 t (1:17), m2 t (1:22), m3 t (1:15), m4 t (2:12), m5 t (4:15), m6 t (3:6), m7 t (8:19), m8 t (9:10), m9 t (9:16), m10 t (13:13), m11 t (14, 14), and m12 t (18:19).

Phenotypic behavior of MDA8788 cell lines

We next assessed the replicative behavior of the established cell lines using Hoechst 33342 fluorescence dye. The doubling time of both MDA8788 cell lines was found to be approximately 40 hours, which was slower than a median doubling time of 26.5 hours in head and neck squamous cancer cell lines (10). To examine the ability of the tumors to grow under anchorage-independent conditions, we conducted soft agar assays on both cell lines. Neither cell line formed colonies after 3 weeks, whereas MDA1386LN cells formed large colonies (Fig. 3A). To test whether the MDA8788 cells are resistant to anoikis (anchorage-dependent programmed cell death), the cells were grown in suspension culture at various time points. Within 72 hours, most of the MDA8788-6 cells died, whereas the MDA8788-7 cells displayed a 30% viability (Fig. 3B). These results suggested that while the SNUC cell lines had behavior characteristics that were reminiscent of squamous cell carcinomas, the lack of growth in soft agar and the relative anoikis sensitivity suggested a more epithelial-like phenotype. To examine the migratory and invasive potential of the SNUC cells, the MDA8788-6 cells were evaluated by *in vitro* Transwell migration and invasion assays. MDA8788-6 did not migrate or invade, even after 48 hours, whereas OSC19 showed both invasion and migration (Supplementary Fig. S2).

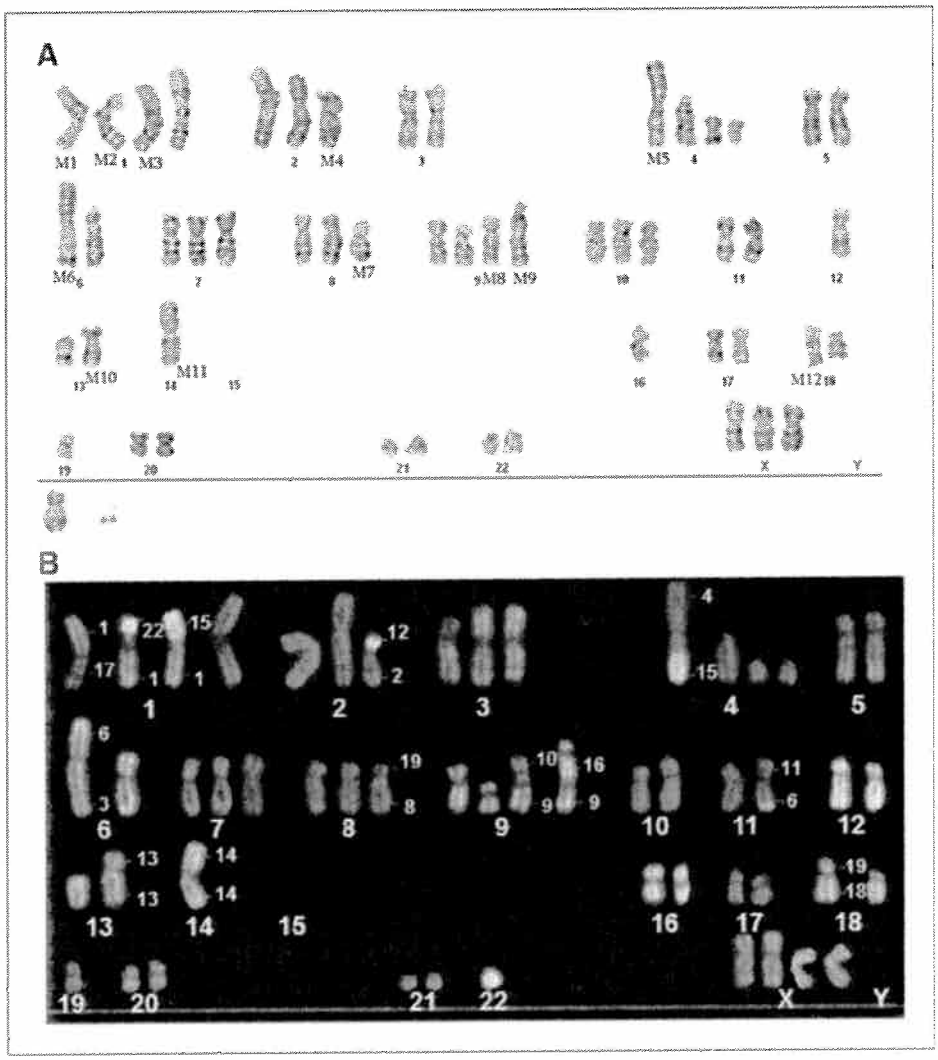

Figure 2. Cytogenetic analysis of the MDA8788-6 cell line. Representative G-banding (A) and spectral karyotyping (SKY) karyotyping (B) results for MDA8788-6 cells showing structural rearrangements.

Published OnlineFirst on October 2, 2012; DOI:10.1158/1078-0432.CCR-12-1876

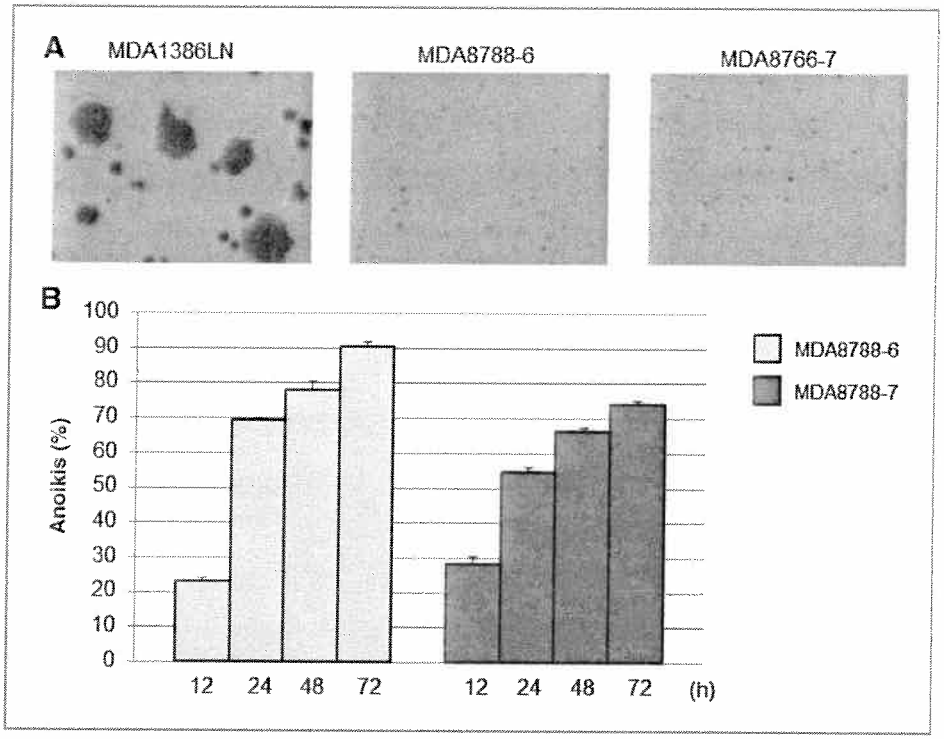

Figure 3. Anchorage-dependent growth in MDA8788 cells. A, colony formation assay was conducted in 0.3% soft agar. No colonies were observed in the MDA8788 cell lines after 3 weeks of culture. The MDA1386LN cell line was used as a positive control and formed large colonies. B, anoikis assay in MDA8788 cells. A total of 2×10^6 trypsinized cells in 10-mL of culture media in a 15-mL tube were cultured with rotation. Cell viability was examined by staining with 0.2% Trypan blue. By 72 hours, most of the MDA8788-6 cells underwent apoptosis, whereas the MDA8788-7 line was slightly more resistant to anoikis.

Epithelial–mesenchymal transition and neuroendocrine markers in SNUC cells

As SNUC tumors display both epithelial and mesenchymal biologic features, we next sought to examine whether the established SNUC cells express epithelial and mesenchymal markers by Western blotting (Fig. 4A). Both MDA8788 cells displayed high expression of pan-keratin, whereas the original tumor specimen had minimum expression compared with the SNUC cell lines, OSC19 (used as a positive control) and UMSCC33 (used as a representative of squamous cell carcinoma from the maxillary sinus). To specify the types of cytokeratin the SNUC cells were expressing, 2 antibodies recognizing cytokeratin 8 and 19 were used for Western blotting. Our SNUC tumor specimen and cell lines were positive for both cytokeratins.

The MDA8778 cell lines also expressed the epithelial markers E-cadherin and β-catenin but not the mesenchymal markers N-cadherin, vimentin, or α-SMA (Fig. 4A). The expression pattern of the EMT markers did not change during the course of cell culture (Supplementary Fig. S3). On the other hand, the SNUC tumor was positive for all the markers including the mesenchymal markers (Fig. 4A). To determine the origin of these mesenchymal markers seen in Western blotting, we conducted an immunohistochemical analysis of surgical specimen. Examination of H&E stained SNUC specimen revealed areas of epithelial tumor as well as nontumor components including stroma (Supplementary Fig. S4A). The areas of tumor expressed epithelial markers (keratins and E-cadherin; Supplementary Fig. S4B and S4C, respectively) but did not express mesenchymal markers. On the other hand, the nontumor area expressed mesenchymal markers (α-SMA and vimentin, Supplementary Fig. S4D and S4E, respectively) but did not express epithelial markers. Because SNUC is a neuroendocrine tumor, we also studied the expression level of synaptophysin. Neither the original tumor nor the MDA8788 cell lines showed any synaptophysin staining (Fig. 4B), which is consistent with the immunohistochemical profile conducted on the original tumor (data not shown).

Tumorigenicity of MDA8788 cells in nude mice

To determine whether the SNUC cell lines were tumorigenic *in vivo*, viable cells were injected into the flanks of nude mice with or without Matrigel. Both MDA8788-6 and MDA8688-7 cells formed tumors (Fig. 5A and Supplementary Fig. S5A, respectively), whereas Matrigel substantially enhanced the tumor growth statistically significantly by day 39 in MDA8788-6 and day 28 in MDA8788-7 ($P < 0.005$; Fig. 5B–D and Supplementary Fig. S5B and S5C, respectively). Histopathologic examination of the tumors revealed minimal differences in morphologic characteristics between tumors of mice injected with or without Matrigel (data not shown). As expected, the tumors grown from both MDA8788-6 and MDA8788-7 cells (Fig. 5E and Supplementary Fig. S5D, respectively) had a histopathologic appearance similar to that of the original surgical specimen (Fig. 1B), although the tumors from the MDA8788-7 line had a slightly more squamoid appearance than that of the MDA8788-6 line. Metastases were not identified in any of the mice at necropsy (data not shown).

Published OnlineFirst on October 2, 2012; DOI:10.1158/1078-0432.CCR-12-1876

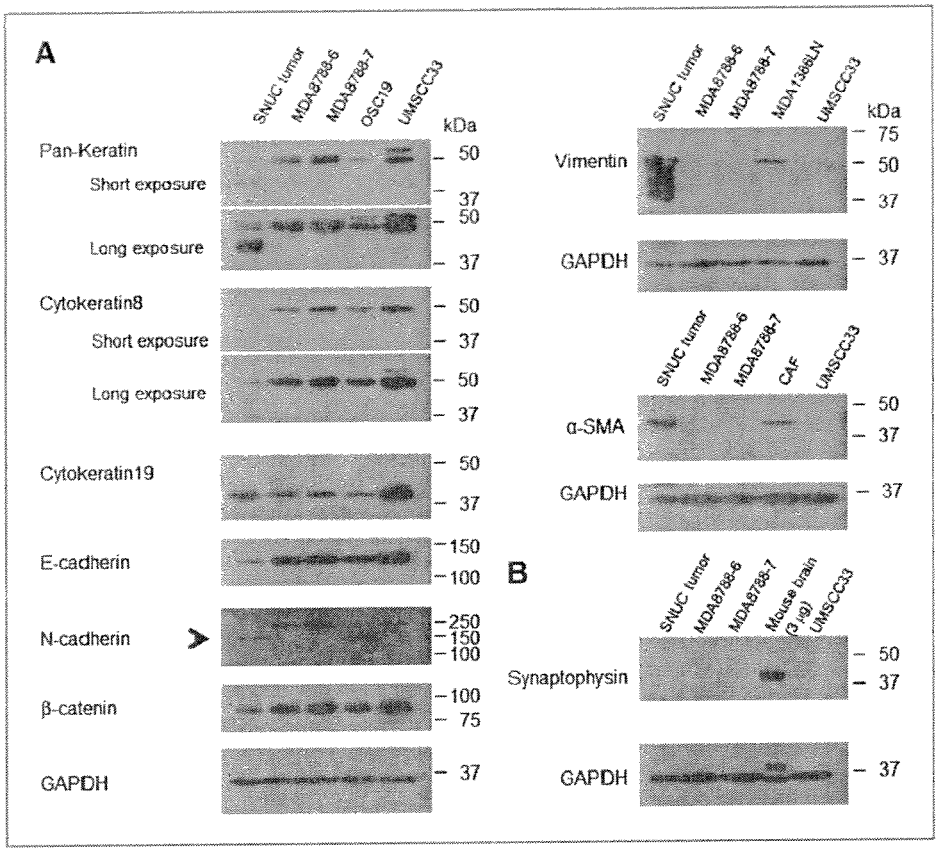

Figure 4. Expression pattern of epithelial–mesenchymal transition and endocrine markers in SNUC cells. Expression pattern of various epithelial and mesenchymal markers was analyzed by Western blotting. A, the original tumor and the 2 MDA8788 cell lines expressed epithelial markers (pan-keratin, cytokeratin 8, cytokeratin 19, E-cadherin, and β-catenin) but did not express mesenchymal markers (N-cadherin, vimentin, and α-SMA). Cell lines used for positive controls were OSC19 (for pan-keratin, cytokeratins 8 and 19, E- and N-cadherins, and β-catenin), MDA1386LN (for vimentin), and cancer-associated fibroblast (CAF; for α-SMA). The arrowhead shows the molecular weight corresponding to N-cadherin. B, synaptophysin expression was negative in the original tumor and both MDA8788 cell lines. Total brain lysate from a mouse was used as a positive control. UMSCC33 was used as a representative of sinonasal squamous cell carcinoma. GAPDH, glyceraldehyde-3-phosphate dehydrogenase.

Orthotopic skull base model of MDA8788 cells

To examine whether the SNUC cells represent clinical features, we injected MDA8788-6 cells into the soft palate of mice. The implanted cells developed visible tumors in nude mice and tumor invasion into the brain was observed by a T_1 -weighted image (Fig. 6A and B). Staining with H&E showed local invasion into muscle (Fig. 6C), bone (Fig. 6D), nerve (Fig. 6E), blood vessels (Fig. 6F), and lymphatic vessels (Fig. 6G). The *in vivo* behavior accurately reflected the invasive nature of SNUC tumors in patients.

Discussion

The aim of this study was to establish a reliable and phenotypically accurate tumor model system for SNUC, and we were successful in establishing and characterizing 2 novel isogenic SNUC cell lines. Malignant sinonasal tumors are clinically challenging because of their rarity, their proximity to vital structures, and their histologic variety within a complex anatomic region. These tumors comprise fewer than 3.6% of all malignancies seen in the head and neck (17). Among them, SNUC is particularly rare and aggressive. It was first described by Frierson and colleagues in 1986 (1), and fewer than 100 cases had been reported by 2005 (18). Despite multimodality therapy, including surgical resection, chemotherapy, and radiotherapy, the prognosis for patients with SNUC is poor; the median survival is less than 18 months (2, 3) and the 5-year survival rate is less than 20% (19).

The development and evaluation of new therapeutic approaches for SNUC has been limited by a lack of available models. To better understand and overcome the poor outcomes of patients diagnosed with this disease, establishment of a tumor model of SNUC is essential. Currently, there are few cell lines derived from sinonasal tumors; most of them were isolated from squamous cell carcinomas (9, 10) and one was established from an intestinal-type sinonasal adenocarcinoma (20). No stable SNUC cell lines had been reported before the development and characterization of the cell lines reported here. These new cell lines are designated MDA8788-6 and MDA8788-7, and they were derived from a T4N0M0 SNUC of the right maxillary sinus of a 74-year-old female who was diagnosed and treated at our center. STR genotyping analysis revealed the isogenic nature of the 2 MDA8788 cell lines and the parent tumor. The morphologic features of the cells were stable throughout cell culture. These results indicate that our newly established cell lines are representative of the disease, making them useful for preclinical studies of the biology and treatment of SNUC.

An analysis by Gil and colleagues showed that 30% of the SNUCs have an abnormal karyotype. In our study, 12 chromosomal translocations were identified in both MDA8788 cell lines. None of these translocations matched with previous cytogenetic studies of SNUCs (21, 22). It will be interesting to investigate the functional impact of the observed chromosomal translocations as studies in other

Published OnlineFirst on October 2, 2012; DOI:10.1158/1078-0432.CCR-12-1876

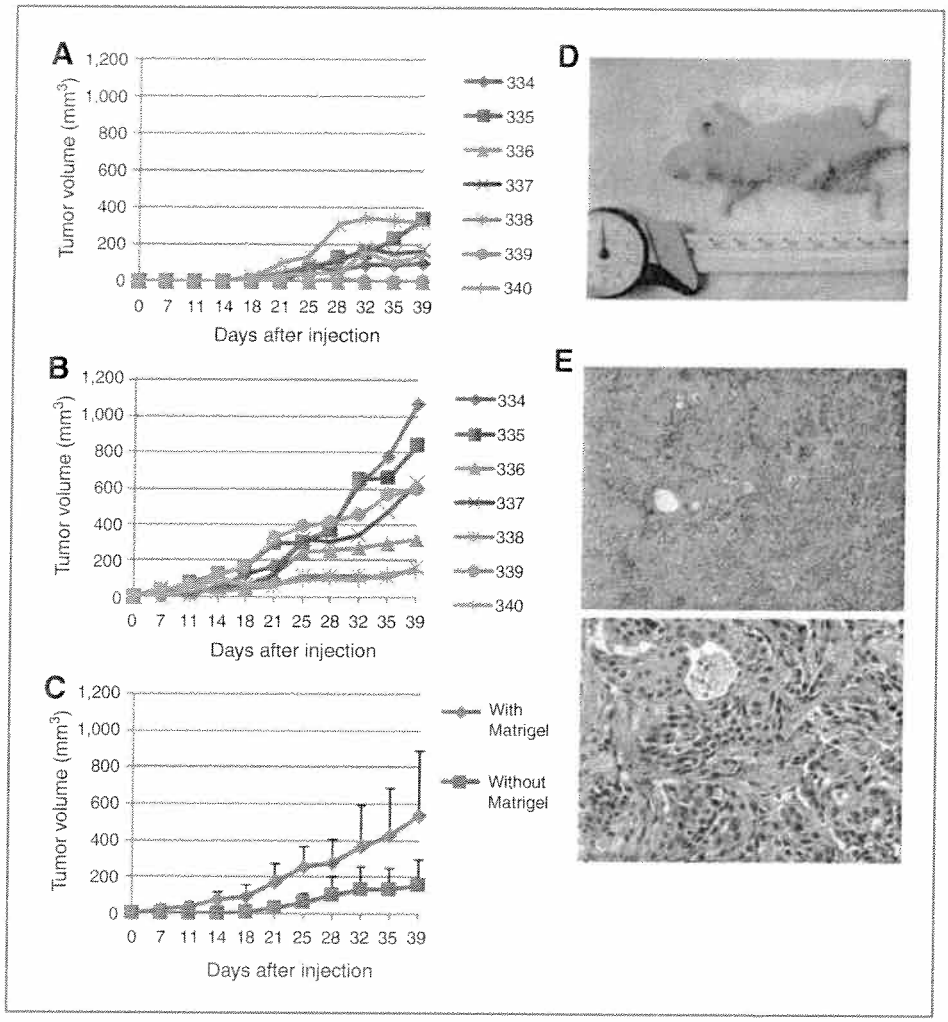

Figure 5. Heterotransplantation of MDA8788-6 cells into nude mice. Tumorigenicity was examined by injecting cells into the flanks of the mice. Each color in A and B indicates identification number of the mice. A, the cells injected into the flanks without Matrigel formed tumors in 66% of mice (4 of 6 mice). B, by adding Matrigel, tumors grew larger and faster than the ones without adding Matrigel. Tumor formation was observed in 100% of animals. C, mean tumor sizes. D, appearance of a subcutaneous MDA8788-6 tumor in a nude mouse. The cells were injected into the right flank without Matrigel and into the left flank with Matrigel. E, the tumors from MDA8788-6 had a similar histopathologic appearance as that of the original surgical specimen [H&E staining; original magnifications ×40 (top) and ×200 (bottom)].

tumor types have identified oncogenic activation of proto-oncogenes at chromosomal breakpoints. Further analysis of the observed cytogenetic abnormalities with mutational studies may yield potential molecular targets in this disease.

We found it interesting that despite the highly aggressive nature of SNUC in patients, the SNUC cell lines showed a less malignant phenotype in tumor models. For example, the doubling time of the cells was relatively slow, they did not form colonies in soft agar, and they were relatively sensitive to detachment. They did not migrate or invade in *in vitro* assays. On the other hand, the SNUC cells were highly tumorigenic in the mice. To determine the tumorigenic potential of the MDA8788 cell lines, the cells were heterotransplanted into nude mice. The cells formed solid tumors histologically identical to the original surgical specimen, indicating that our SNUC cell lines can be used as reliable reagents for *in vivo* preclinical studies. These findings indicate that the microenvironment of the tumor may play an important role for the development of SNUCs. Moreover, *in vitro* experiments may be less revealing, *vis-à-vis* potential therapeutic targets and, thus, well-designed animal studies may be required in this unique disease. It is known that SNUC presents as large tumors involving multiple sinonasal structures, often extends into the orbital or cranial cavity, and can metastasize to the cervical lymph nodes, lungs, bones, brain, and liver (2, 4–6). To determine the reliability of our SNUC cell lines in replicating phenotype of SNUC in patients, the cells were orthotopically implanted to mice. Histologic examination showed that developed tumors could invade into the nasal cavity and cranial cavity, indicating that these SNUC cell lines and the orthotopic model may work as powerful preclinical tools.

Immunoblotting assay revealed that MDA8788 cells were positive for pan-keratin, cytokeratin 8, and cytokeratin 19, which are positive in SNUC specimens at high rates (4, 8, 23–26). Other epithelial markers and mesenchymal markers were also tested. The SNUC cell lines were also found to express the epithelial markers E-cadherin and β-catenin, but they do not express the mesenchymal markers N-cadherin, vimentin, or α-SMA, indicating that the SNUC cell lines have epithelial characteristics and not mesenchymal features. Interestingly, our SNUC specimen expressed the epithelial markers at lower levels than the SNUC cell lines and was positive for the mesenchymal

Published OnlineFirst on October 2, 2012; DOI:10.1158/1078-0432.CCR-12-1876

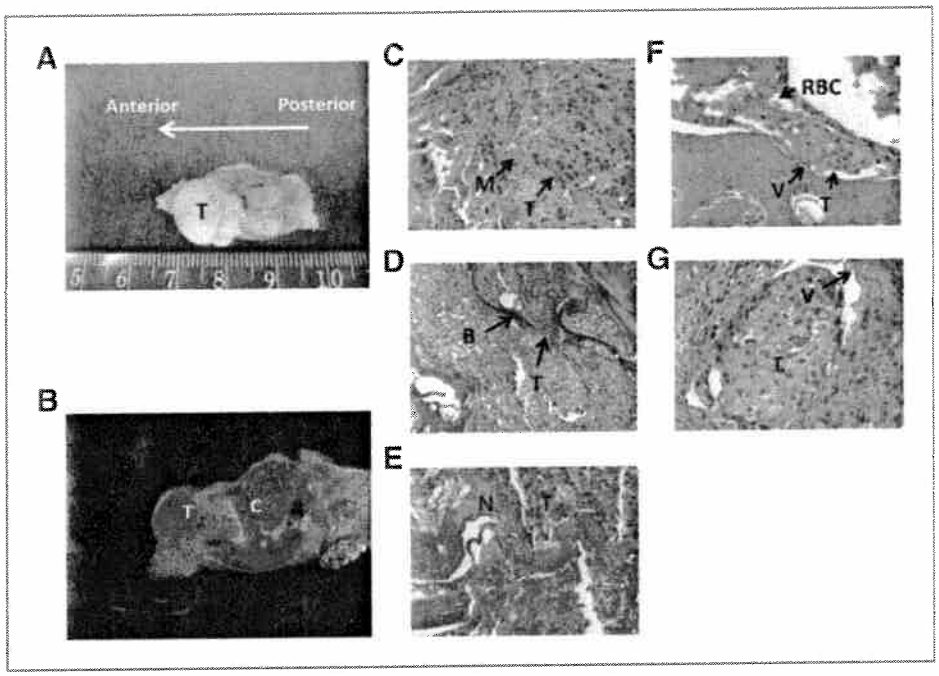

Figure 6. Orthotopic transplantation of MDA8788-6 cells into nude mice. A, sagittal MRI of a tumor from the human MDA8788-6 SNUC line that had been implanted in the soft palate of a mouse. C, cerebrum; T, tumor. B. MRI of serial axial images 12 days after the injection. C–G, H&E staining shows several types of invasions. B, bone; M, muscle; N, nerve; RBC, red blood cells; T, tumor; V, vessel (original magnification, ×200). Muscle invasion (C), bone invasion (D), perineural invasion (E), vascular invasion (F), and lymphovascular invasion (G).

markers. This may be the result of contamination of non tumor cells, such as cancer-associated fibroblasts. Neither the surgical specimen nor the SNUC cells expressed synaptophysin, despite this tumor's neuroendocrine classification. Some researchers have already reported that SNUC can often be synaptophysin-negative consistent with our finding (4, 8, 23, 27).

In summary, this is the first report of establishing stable human-derived SNUC cell lines. The cell lines are highly tumorigenic and maintain the histologic and molecular features of the original tumor when grown in murine models. Therefore, these lines may serve as useful tools for future studies of SNUC tumor biology, as well as in the development and testing of novel therapies for this deadly disease.

Disclosure of Potential Conflicts of Interest

No potential conflicts of interest were disclosed.

Authors' Contributions

Conception and design: Y. Takahashi, M.E. Kupferman, M.J. Frederick, J.N. Myers, E.Y. Hanna

Development of methodology: Y. Takahashi, M.E. Kupferman, M. Zhao, J. N. Myers, E.Y. Hanna

Acquisition of data (provided animals, acquired and managed patients, provided facilities, etc.): Y. Takahashi, M.E. Kupferman, D. Bell, T. Jiffar, J. G. Lee, T.-X. Xie, N.-W. Li, A. Gelbard, J.N. Myers, E.Y. Hanna

Analysis and interpretation of data (e.g., statistical analysis, biostatistics, computational analysis): Y. Takahashi, M.E. Kupferman, D. Bell, J. G. Lee, T.-X. Xie, N.-W. Li, A. Gelbard, J.N. Myers

Writing, review, and/or revision of the manuscript: Y. Takahashi, M.E. Kupferman, T. Jiffar, N.-W. Li, J.N. Myers, E.Y. Hanna

Administrative, technical, or material support (i.e., reporting or organizing data, constructing databases): M.E. Kupferman, T. Jiffar, M. Zhao, J.N. Myers

Study supervision: M.E. Kupferman, J.N. Myers, E.Y. Hanna

Acknowledgments

The authors thank Drs. T.J. Liu and Yoshitsugu Mitani for providing technical support, Samar Jasser and Terri Astin for administrative assistance, and Lizzie Hess for her important editing of the manuscript.

Grant Support

This work was supported by the Pittsburgh Foundation Study of Sinonasal Malignancies, Various Donors Sinus Cancer Research Fund, The University of Texas MD Anderson Cancer Center institutional start-up funds (179475 and 179495), a National Cancer Institute-Cancer Center Core Grant (NCI CA16672), NIH Grant K08-DE019185 (M.E. Kupferman), Joint American-College of Surgeons – Triological Society Clinical Scientist Development Award (M.E. Kupferman), and Sheila Newar Cancer Research Fund (M.E. Kupferman).

The costs of publication of this article were defrayed in part by the payment of page charges. This article must therefore be hereby marked *advertisement* in accordance with 18 U.S.C. Section 1734 solely to indicate this fact.

Received June 11, 2012; revised September 12, 2012; accepted September 14, 2012; published OnlineFirst October 2, 2012.

References

1. Frierson HF Jr, Mills SE, Fechner RE, Taxy JB, Levine PA. Sinonasal undifferentiated carcinoma. An aggressive neoplasm derived from schneiderian epithelium and distinct from olfactory neuroblastoma. Am J Surg Pathol 1986;10:771–9.
2. Cerilli LA, Holst VA, Brandwein MS, Stoler MH, Mills SE. Sinonasal undifferentiated carcinoma: immunohistochemical profile and lack of EBV association. Am J Surg Pathol 2001;25:156–63.
3. Jeng YM, Sung MT, Fang CL, Huang HY, Mao TL, Cheng W, et al. Sinonasal undifferentiated carcinoma and nasopharyngeal-type undifferentiated carcinoma: two clinically, biologically, and histopathologically distinct entities. Am J Surg Pathol 2002;26:371–6.
4. Ejaz A, Wenig BM. Sinonasal undifferentiated carcinoma: clinical and pathologic features and a discussion on classification, cellular differentiation, and differential diagnosis. Adv Anat Pathol 2005;12:134–43.

Published OnlineFirst on October 2, 2012; DOI:10.1158/1078-0432.CCR-12-1876

5. Ghosh S, Weiss M, Streeter O, Sinha U, Commins D, Chen TC. Drop metastasis from sinonasal undifferentiated carcinoma: clinical implications. Spine (Phila Pa 1976) 2001;26:1486–91.
6. Mendenhall WM, Mendenhall CM, Riggs CE Jr, Villaret DB, Mendenhall NP. Sinonasal undifferentiated carcinoma. Am J Clin Oncol 2006;29:27–31.
7. Tanzler ED, Morris CG, Orlando CA, Werning JW, Mendenhall WM. Management of sinonasal undifferentiated carcinoma. Head Neck 2008;30:595–9.
8. Smith SR, Som P, Fahmy A, Lawson W, Sacks S, Brandwein M. A clinicopathological study of sinonasal neuroendocrine carcinoma and sinonasal undifferentiated carcinoma. Laryngoscope 2000;110:1617–22.
9. Liebertz DJ, Lechner MG, Masood R, Sinha UK, Han J, Puri RK, et al. Establishment and characterization of a novel head and neck squamous cell carcinoma cell line USC-HN1. Head Neck Oncol 2010;2:5.
10. Lin CJ, Grandis JR, Carey TE, Gollin SM, Whiteside TL, Koch WM, et al. Head and neck squamous cell carcinoma cell lines: established models and rationale for selection. Head Neck 2007;29:163–88.
11. Pathak S. Chromosome banding techniques. J Reprod Med 1976;17:25–8.
12. Kupferman ME, Patel V, Sriuranpong V, Amornphimoltham P, Jasser SA, Mandal M, et al. Molecular analysis of anoikis resistance in oral cavity squamous cell carcinoma. Oral Oncol 2007;43:440–54.
13. Kupferman ME, Jiffar T, El-Naggar A, Yilmaz T, Zhou G, Xie T, et al. TrkB induces EMT and has a key role in invasion of head and neck squamous cell carcinoma. Oncogene 2010;29:2047–59.
14. Bell D, Roberts D, Karpowicz M, Hanna EY, Weber RS, El-Naggar AK. Clinical significance of Myb protein and downstream target genes in salivary adenoid cystic carcinoma. Cancer Biol Ther 2011;12:569–73.
15. Mullen P. The use of Matrigel to facilitate the establishment of human cancer cell lines as xenografts. Methods Mol Med 2004;88:287–92.
16. Gelbard A, Kupferman ME, Jasser SA, Chen W, El-Naggar AK, Myers JN, et al. An orthotopic murine model of sinonasal malignancy. Clin Cancer Res 2008;14:7348–57.
17. Barnes L. Surgical pathology of the head and neck. Vol 1; 2001. Available from: http://search.ebscohost.com/login.aspx?direct=true&db=nlebk&AN=57141&site=ehost-live.
18. Frierson HF. Sinonasal undifferentiated carcinoma. In:Barnes L, Eveson JW, Reichart P, Sidransky D, editors. Pathology and genetics of head and neck tumors (World Health Organization classification of tumors). Lyon, France: IARC Press; 2005. p. 19.
19. Gallo O, Graziani P, Fini-Storchi O. Undifferentiated carcinoma of the nose and paranasal sinuses. An immunohistochemical and clinical study. Ear Nose Throat J 1993;72:588–90, 593–5.
20. Perez-Escuredo J, Garcia Martinez J, Garcia-Inclan C, Vivanco B, Costales M, Alvarez Marcos C, et al. Establishment and genetic characterization of an immortal tumor cell line derived from intestinal-type sinonasal adenocarcinoma. Cell Oncol (Dordr) 2011;34:23–31.
21. Gil Z, Orr-Urtreger A, Voskoboinik N, Trejo-Leider L, Spektor S, Shomrat R, et al. Cytogenetic analysis of sinonasal carcinomas. Otolaryngol Head Neck Surg 2006;134:654–60.
22. Gil Z, Orr-Urtreger A, Voskoboinik N, Trejo-Leider L, Shomrat R, Fliss DM. Cytogenetic analysis of 101 skull base tumors. Head Neck 2008;30:567–81.
23. Bellizzi AM, Bourne TD, Mills SE, Stelow EB. The cytologic features of sinonasal undifferentiated carcinoma and olfactory neuroblastoma. Am J Clin Pathol 2008;129:367–76.
24. Bourne TD, Bellizzi AM, Stelow EB, Loy AH, Levine PA, Wick MR, et al. p63 Expression in olfactory neuroblastoma and other small cell tumors of the sinonasal tract. Am J Clin Pathol 2008;130:213–8.
25. Franchi A, Moroni M, Massi D, Paglierani M, Santucci M. Sinonasal undifferentiated carcinoma, nasopharyngeal-type undifferentiated carcinoma, and keratinizing and nonkeratinizing squamous cell carcinoma express different cytokeratin patterns. Am J Surg Pathol 2002;26:1597–604.
26. Wenig BM. Undifferentiated malignant neoplasms of the sinonasal tract. Arch Pathol Lab Med 2009;133:699–712.
27. Cordes B, Williams MD, Tirado Y, Bell D, Rosenthal DI, Al-Dhahri SF, et al. Molecular and phenotypic analysis of poorly differentiated sinonasal neoplasms: an integrated approach for early diagnosis and classification. Hum Pathol 2009;40:283–92.